RadioGraphics

Vascular Emergencies of the Thorax after Blunt and Iatrogenic Trauma: Multi–Detector Row CT and Three-dimensional Imaging[1]

LEARNING OBJECTIVES

After reading this article and taking the test, the reader will be able to:

■ List the imaging appearances of and differential diagnoses for acute vascular injuries of the thorax.

■ Discuss the values of the different imaging modalities for diagnosis of various aortic syndromes.

■ Describe the clinical and CT features of conditions due to iatrogenic vascular trauma of the thorax.

Hatem Alkadhi, MD • Simon Wildermuth, MD • Lotus Desbiolles, MD
Thomas Schertler, MD • David Crook, MD • Borut Marincek, MD
Thomas Boehm, MD

Multi–detector row computed tomographic (CT) angiography is an effective modality for vascular imaging in the thorax. It allows acquisition of high-resolution data sets during a single breath hold, making it the preferred method for evaluation of patients with acute vascular disease. In contrast to conventional angiography, multirow CT angiography not only depicts the vessels but also allows assessment of adjacent structures. Multirow CT angiography with two- and three-dimensional reformation can be used to diagnose vascular emergencies of the thorax after blunt and iatrogenic trauma. These include incomplete and complete aortic rupture; traumatic aortic dissection; arterial dissection and rupture after minor trauma in patients with Ehlers-Danlos syndrome; traumatic intramural hematoma; pseudoaneurysm after endovascular repair; injuries due to Swan-Ganz catheters; complications of central venous cannulation, pacemaker implantation, and percutaneous pericardial drainage; and foreign-body embolism. The diagnoses can be established with multirow CT angiography in the emergency department. Thus, the time to diagnosis can be considerably decreased by obviating conventional angiography. Knowledge of the CT findings in various vascular conditions is essential to make use of multirow CT angiography in combination with two- and three-dimensional reformation as an efficient and accurate diagnostic tool in emergency radiology.

©RSNA, 2004

Introduction

Computed tomography (CT) is evolving as a key imaging modality for the noninvasive assessment of the vascular system (1). The introduction of multi–detector row CT has offered a number of advantages in the work-up strategy of emergency patients when compared with single-section CT (2). The shorter scanning time permits better opacification of the blood vessels and improved contrast material enhancement of parenchymal organs. Furthermore, faster data acquisitions allow multiple consecutive CT examinations in the same patient in a shorter period of time (2).

The advent of multirow CT not only creates new opportunities but also requires changes in radiologic viewing methods and data handling (3). Multiplanar reformation (MPR), shaded surface display (SSD), maximum intensity projection (MIP), and volume rendering are the most commonly used two- and three-dimensional postprocessing techniques. They may be used as the initial and only imaging modality for assessment of vascular pathologic conditions and for surgical planning, often obviating conventional angiography and hereby leading to reduced costs (4). Furthermore, multirow CT angiography combined with three-dimensional rendering is the preferred tool to plan endovascular interventional treatment at our institute. This includes vessel segmentation for determination of optimal stent-graft dimensions for aortic aneurysms. The follow-up of patients after stent-graft placement, planning of reinterventions after stent-graft displacement, and assessment of the different types of endoleaks are also done by using multirow CT angiography and the different reformation techniques.

Assessment of thoracic vascular emergency is nowadays possible by using multirow CT angiography as a "one-stop shop" strategy. Thorough knowledge of anatomy, pathophysiology, and image rendering techniques, as well as precise description and interpretation of thoracic vascular findings, are therefore essential in establishing the correct diagnosis and avoiding unnecessary and costly interventions.

In this pictorial essay, we illustrate the applications of multirow CT angiography in a variety of thoracic vascular emergencies caused by blunt and iatrogenic trauma. These selected examples highlight the manifold advantages of multirow CT angiography with its improved multiplanar and three-dimensional postprocessing techniques.

Imaging Technique

Optimized protocols are essential in maximizing the yield of diagnostic information for the most complete and accurate CT assessment possible. A specific intravenous contrast material injection protocol must be applied selectively to each vascular region. Therefore, different protocols for each anatomic area and for traumatic and non-traumatic emergency conditions are preprogrammed on the scanner and the contrast material power injector. For optimal assessment of vascular emergencies, collimation, pitch, and intravenous contrast material injection protocols must be tailored to the region of interest for the given anatomic area.

Imaging of thoracic vascular emergencies was performed with a four-row CT scanner (Somatom Volume Zoom; Siemens Medical Solutions, Forchheim, Germany). Details about the scanning protocols are listed in the Table. The radiation exposure was calculated by using a commercially available computer program (WinDose, version 2.1a; Scanditronix-Wellhöfer Dosimetrie, Schwarzenbruck, Germany). The effective radiation dose calculations were based on Monte Carlo calculations for anthropomorphic mathematical phantoms (GSF National Research Center for Environment and Health, Neuherberg, Germany) (5). A 150-mL dose of nonionic contrast material (Visipaque 320 [iodine, 320 mg/mL]; Amersham

Protocol for Multi–Detector Row CT

Phase	Delay after Injection (sec)	Tube Potential (kV)	Effective Tube Current (mAs)	Feed per Rotation (mm)	Rotation Time (sec)	Collimation	Section Width (mm)	RI* (mm)	Radiation Dose (mSv) Female Patient	Radiation Dose (mSv) Male Patient
Arterial	15–25	120	140	6	0.5	4 × 1 mm	1	0.6	4.6	3.5
Venous	65–75	120	140	15	0.5	4 × 2.5 mm	3	2	3.9	3.1

*RI = reconstruction increment.

Health, Buckinghamshire, England) was injected at a rate of 3 mL/sec. C.A.R.E. Bolus (Siemens Medical Solutions), an event-triggering protocol that initiates data acquisition at a predefined level of opacification in a given region of interest, was used to optimize arterial opacification. The region of interest for these measurements was placed in the thoracic descending aorta.

Arterial and venous phase images were then acquired throughout the entire thorax to characterize the arterial blood supply and the venous drainage. Performing a dual-phase examination in the arterial and venous phases may also be beneficial for an exact evaluation of arterial dissections, for the detection of acute bleeding (ie, contrast media extravasation), and for the assessment of possible endoleaks after endovascular stent grafting of acute aortic syndromes. This scanning protocol represents the routine protocol used at our institute for evaluation of patients with acute thoracic trauma in the emergency suite and for follow-up CT examinations after endovascular stent grafting. Electrocardiographically synchronized data acquisition for minimizing cardiac motion artifacts was not employed due to the key limitations of large scan volumes and the resulting increase in scanning time due to requisite pitch reduction (1). Future developments in CT technology and use of the latest-generation CT scanners with more than 16 detector rows should overcome these limitations.

Blunt Trauma

Incomplete Aortic Rupture

Traumatic aortic ruptures after rapid deceleration accidents are thought to result from a number of different mechanical factors, which all contribute to injury (6). They involve a combination of traction, torsion, and hydrostatic forces created by differential deceleration of thoracic structures (6–11).

In approximately 20% of cases, the aortic injury may be limited to a partial circumferential tear in the intima and/or the media of the aortic wall (9,11). If the adventitia remains intact, it may be strong enough to contain the circulation within the aorta, and the individual has a chance of survival. Arterial blood pressure or blood from intramural vasa vasorum can force blood between the layers, forming a false aneurysm or pseudoaneurysm. CT findings typically consist of a saccular outpouching demarcated from the aortic lumen by a collar. This pseudoaneurysm is limited externally by a thin layer of adventitia and by neighboring tissues. The integrity of the adventitia cannot be assessed from CT findings; however, an intact adventitia can be assumed in cases of pseudoaneurysm formation. It is usually surrounded

RadioGraphics

a.

b.

c.

d.

e.
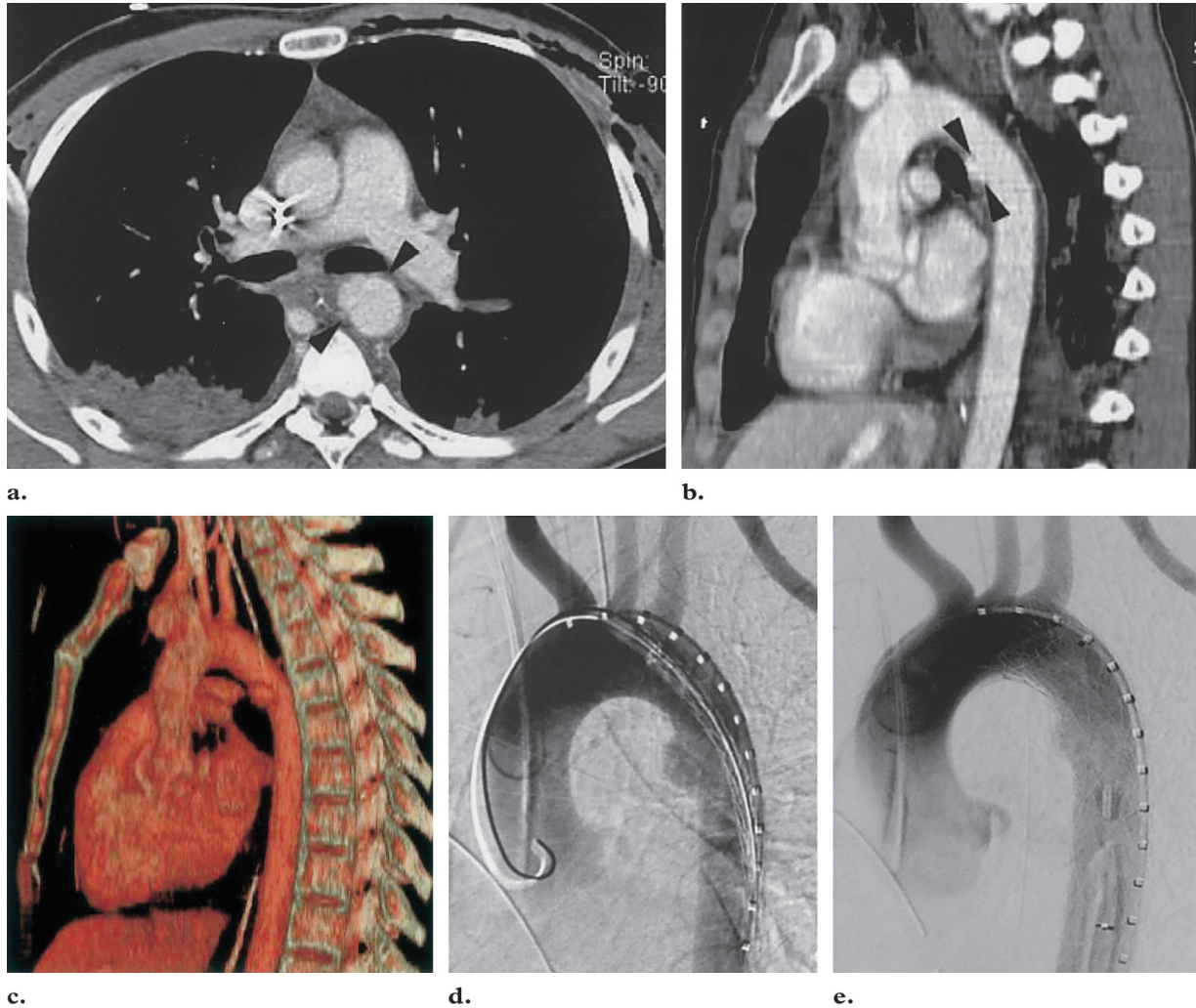
Figure 1. Incomplete rupture of the descending aorta in a 51-year-old man with blunt thoracic trauma from a traffic accident. **(a, b)** Axial CT image **(a)** and oblique sagittal reformatted image **(b)** show a saccular outpouching of the descending aorta. The outpouching is demarcated from the aortic lumen by a collar (arrowheads), and there is only a small periaortic hematoma. The nasogastric tube is not deviated. **(c)** Sagittal volume rendered image shows the pseudoaneurysm more clearly. **(d)** Left anterior oblique angiogram shows endovascular repair of the aneurysm. **(e)** Left anterior oblique angiogram shows that the repair was successful, with preservation of all supraaortic vessels.

by a certain amount of hemomediastinum (Fig 1). If treatment such as endovascular stent grafting is not undertaken, the pseudoaneurysm may eventually rupture and severely threaten the life of the individual.

Complete Aortic Rupture

In severe aortic injury, complete transection results as the tear extends from the intima and media into the adventitial layer (6,9,11). Subsequent mediastinal hemorrhage rapidly extends cranially, leading to left apical extrapleural capping. The mediastinal hematoma may later rupture into the pleural space, resulting in a left-sided hemothorax. Massive mediastinal and pleural hemorrhage usually leads to immediate death (8).

Approximately 90% of blunt traumatic aortic injuries occur at the anteromedial aspect of the aortic isthmus distal to the origin of the left subclavian artery. Seven percent to 8% of blunt traumatic aortic lesions are located in the aortic root (7,8,10) and are often associated with aortic valve tears, cardiac contusions or ruptures, coronary artery tears, and/or hemopericardium with cardiac tamponade. In nearly 2% of cases, blunt traumatic lesions of the descending aorta occur at the level of the diaphragm (7,8,10). In 10% of cases they are observed simultaneously with diaphragmatic ruptures, as the biomechanical mechanism of injury is similar (9).

The classic appearance of the ruptured isthmus at contrast-enhanced CT features a sleeve of subadventitial contrast medium. In some cases, a tear involving all three layers can be visualized

a.

b.

c.

d.

e.
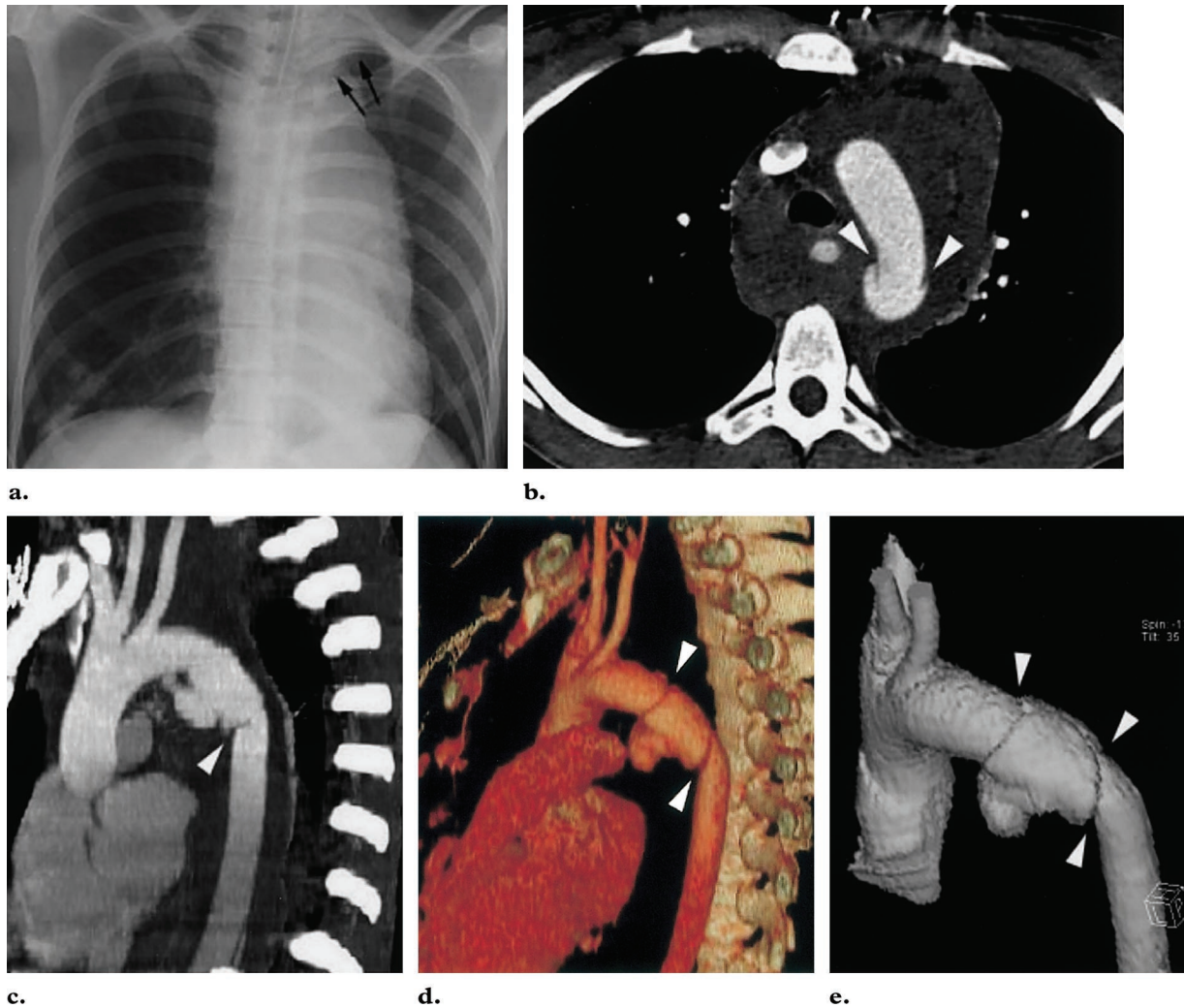
Figure 2.   Complete aortic rupture in a 48-year-old woman with blunt thoracic trauma from a skydiving accident. The lesion was successfully repaired at surgery; however, the patient subsequently died due to severe brain injury. **(a)** Anteroposterior chest radiograph shows a widened upper mediastinum with a faint left apical extrapleural cap (arrows). **(b)** Axial CT image of the aortic isthmus shows complete transection of the aortic wall (arrowheads) with a periaortic hematoma and hemomediastinum. **(c)** Sagittal thin-slab MIP image shows a second, more caudal site of aortic transection (arrowhead) and active mediastinal bleeding. Note the common origin of the brachiocephalic trunk and the left common carotid artery. **(d, e)** Sagittal volume rendered image **(d)** and oblique shaded surface display image **(e)** show both sites of aortic transection (arrowheads) and blood extravasation, thereby facilitating surgical or endovascular intervention.

(Fig 2). CT also accurately shows hemomediastinum and hemothorax, which may be indirect signs of a blunt traumatic aortic lesion. The location of the hemomediastinum is of diagnostic significance: Hemorrhage surrounding the aorta and other vascular structures is more suggestive of vascular injury than, for example, blood that is confined to the retrosternal space adjacent to a sternal fracture. The use of multirow CT angiography in the detection of blunt traumatic aortic lesions has been reported to have a sensitivity, specificity, and accuracy of 96%, 99%, and 99%, respectively (12–15). An unequivocally normal mediastinum at CT with no hematoma and a regular aorta surrounded by normal fat has a 100% negative predictive value for aortic injury (12–15).

Traumatic Aortic Dissection

Aortic dissection is less commonly found in the setting of blunt thoracic trauma (16–22). In the largest series of aortic trauma cases in which a frequency of aortic dissection could be calculated, six dissections (11%) were found in 54 cases of traumatic aortic tears (20). In the most recent study, Perchinsky et al (21) found four

RadioGraphics

Figure 3.   Complex aortic dissection and bilateral hemothorax in a 44-year-old woman with blunt thoracic trauma from a motorcycle accident. **(a)** Axial CT image of the aortic arch shows the intimomedial flap, which divides the aorta into true *(T)* and false *(F)* lumina. **(b)** Axial CT image of the aortic arch shows the intimal entrance tear (arrow). **(c, d)** Oblique thin-slab MIP images show the origin of the dissection and its extension to the left common carotid artery (arrow in **c**) and the brachiocephalic trunk (arrowhead in **d**).

a.

b.

c.

d.
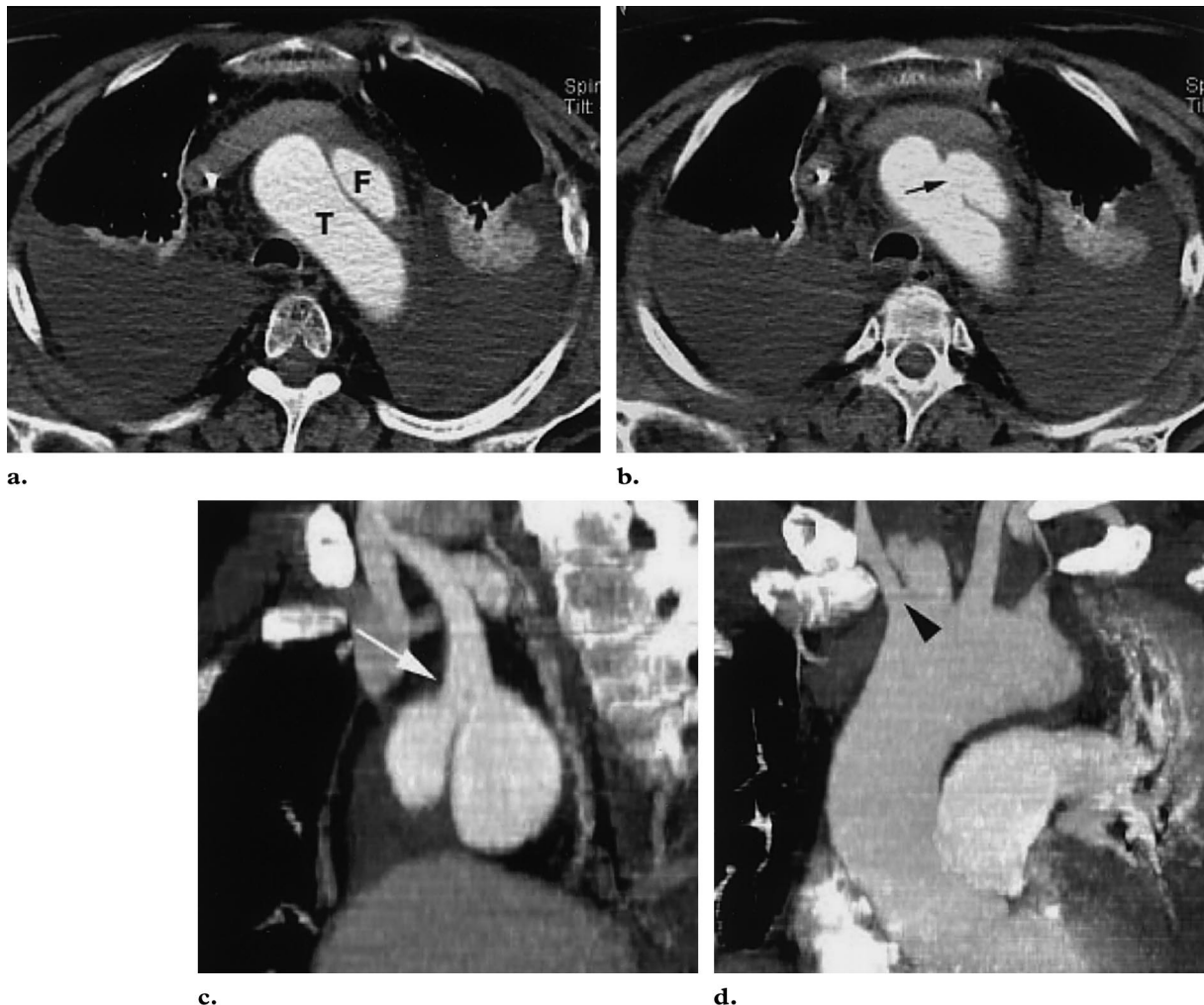
dissections (12%) in 33 patients with traumatic aortic rupture. It is thought that acute hypertension and steepness of the pulse wave along with the rapid deceleration may cause intimal tears and assist in the distal propagation of the dissection (17,18,21,22). Shearing of the vasa vasorum has also been hypothesized as an important initiator of traumatic dissection of the aorta, and increasing age and atherosclerosis have been thought to represent important predisposing factors (20,21).

Whereas spontaneous dissections are typically medially and circumferentially propagating, those resulting from trauma can apparently be both medial and subadventitial as well as longitudinally propagating (17,22,23). The CT signs of traumatic aortic dissection are similar to those of the nontraumatic type. The imaging hallmark is the identification of the intimal flap, which separates the aorta into a true lumen and false lumen (Fig 3). The diagnostic accuracy of multirow CT angiography for the detection of dissections of the thoracic aorta has been shown to be 100% (24).

Arterial Dissection and Rupture after Minor Trauma

The Ehlers-Danlos syndrome is one of the most frequent inherited connective tissue disorders. It is characterized by increased elasticity of the skin, hypermobile joints, easy "bruisability," and excessive gaping of wounds after minor trauma. On the basis of clinical presentation, genetics, and biochemical structure, at least 10 distinct varieties have been recognized (25). In type IV, the so-called arterial-ecchymotic type, the underlying pathologic process is based on defective type III collagen synthesis. Pathologic examination of the arteries shows a disorganized media with fragmented

Figure 4. **(a–c)** Arterial dissection after minor thoracic trauma in a 23-year-old patient with type IV Ehlers-Danlos syndrome. **(a)** Axial CT image of the origin of the left subclavian artery shows an intimomedial flap, which divides the artery into true *(T)* and false *(F)* lumina. **(b)** Axial CT image shows a crescent-shaped intramural hematoma (arrowheads) surrounding the true lumen. **(c)** Sagittal volume rendered image shows a dissection of the proximal descending aorta (type B dissection) (arrow). The dissection extends into the origin of the left subclavian artery. **(d, e)** Arterial rupture after minor thoracic trauma in a 19-year-old patient with type IV Ehlers-Danlos syndrome. **(d)** Coronal thin-slab MIP image shows a ruptured aneurysm of the left subclavian artery (arrow), which caused left-sided hemothorax. There is also a nonruptured, partially calcified aneurysm of the right subclavian artery. This aneurysm was asymptomatic and was probably chronic. **(e)** Oblique coronal volume rendered image from the arterial phase includes only the arterial vessels and thus shows the aneurysms more clearly.

a.

b.

c.

d.

e.
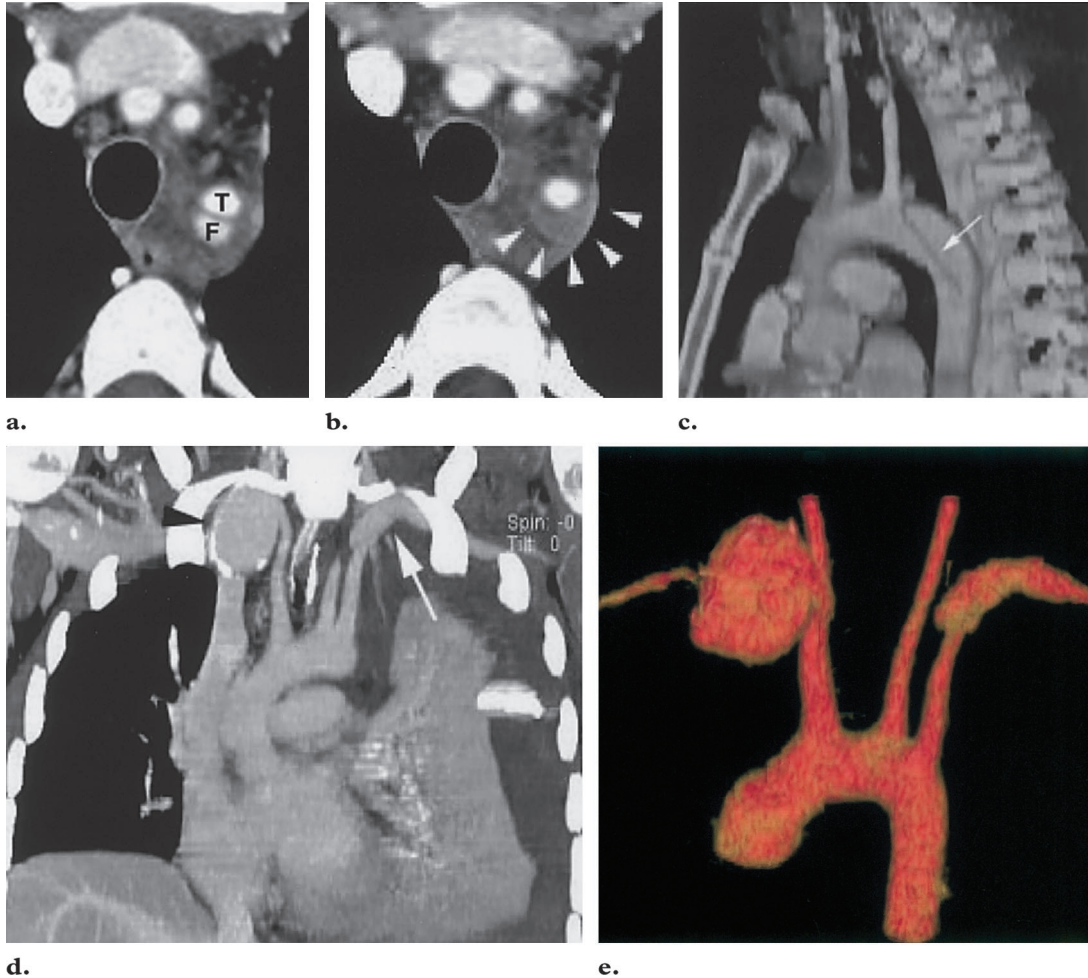
elastic fibers, decreased or absent elastin, irregular medial hyperplasia, and increased ground substance in the inner half of the media (25).

Vascular complications of type IV Ehlers-Danlos syndrome include arteriovenous fistula, aneurysmal rupture, and aneurysmal degeneration with subsequent rupture or dissection. These complications have been reported to occur spontaneously or after minor trauma. Invasive diagnostic procedures such as conventional catheter angiography have a reported complication rate of 67% (26), which underlies the need for noninvasive techniques such as multirow CT angiography to reduce the iatrogenic morbidity in this patient population.

The diagnosis of Ehlers-Danlos syndrome is based on the presence of several major and/or minor criteria (27). One of the major diagnostic criteria of type IV Ehlers-Danlos syndrome (ie, arterial rupture) can be reliably diagnosed with multirow CT angiography. Corresponding to the range of vascular abnormalities, the encountered CT findings include all of the vascular lesions mentioned earlier, such as complete and incomplete arterial rupture, intramural hematoma, and dissection (Fig 4).

Traumatic Acute Intramural Hematoma

The classic aortic dissection is characterized by an intimomedial tear (28,29). However, necropsy data have shown that in nearly 5% of patients with dissection it is not possible to locate an entry tear (30). In the clinical setting, some authors have also noted the absence of an entrance tear in a small proportion of patients with dissection studied with noninvasive imaging techniques. This variant of dissection (noncommunicating aortic dissection) has been referred to as *acute intramural hematoma* (30,31).

In these cases, the false lumen is created by a hemorrhage into the aortic media, most likely after rupture of the vasa vasorum that penetrate the outer half of the media from the adventitia and arborize at this level (28,29,32). This noncommunicating form of aortic dissection has been increasingly reported with modern diagnostic imaging techniques. In patients with traumatic acute intramural hematoma, the thickening of the aortic wall is generally circular (30). Acute intramural hematoma weakens the aorta and may progress either to rupture of the aortic wall externally or to inward disruption of the intimal layer, the latter leading to a communicating aortic dissection (29).

Both CT and transesophageal echocardiography have a high sensitivity and specificity for the diagnosis of acute intramural hematoma. Transesophageal echocardiography has a sensitivity of 97% and a specificity of 100%, whereas angiography has been shown to be less sensitive (83%) (specificity, 100%) because it may fail to demonstrate changes in the media in the absence of an intimal lesion (33). Multirow CT angiography

has been reported to approach a sensitivity of 100% and a negative predictive value of 100% (34,35). At CT, acute intramural hematoma can be distinguished from mural thrombus by identification of the intima: A mural thrombus lies on top of the intima, which is frequently calcified, whereas an intramural hematoma is subintimal (29). The intramural hematoma is usually hyperattenuating at unenhanced CT and hypoattenuating compared to the vessel lumen at contrast material–enhanced CT (Fig 5).

Iatrogenic Trauma

Pseudoaneurysm after Endovascular Repair

Endovascular stent grafting has emerged as a less invasive therapeutic alternative for treating aneurysms of the descending thoracic aorta (36). Growing experience in endovascular surgery as well as continuous refinements in prosthetic equipment have increased the feasibility of this novel technique in selected patients. Although early results are comparing favorably with those of conventional open surgery, several procedure-related complications have been described, such as stent-graft dislodgment, migration, stent fracture, changes in the size and shape of the aorta, and arterial wall injury (37–40). Arterial wall injury can result in acute retrograde aortic dissection or pseudoaneurysm formation (40), necessitating urgent surgical replacement of the ascending aorta and aortic arch.

Although pseudoaneurysm formation at conventional anastomotic sites is a recognized complication, it is rarely seen with endografts. In cases where the pseudoaneurysm is located far from the free edge of the stent-graft, different hypotheses have been proposed as underlying causes. These include altered hydraulic stresses causing a new intimal defect in the aortic wall or an iatrogenic

a.

b.

c.

d.
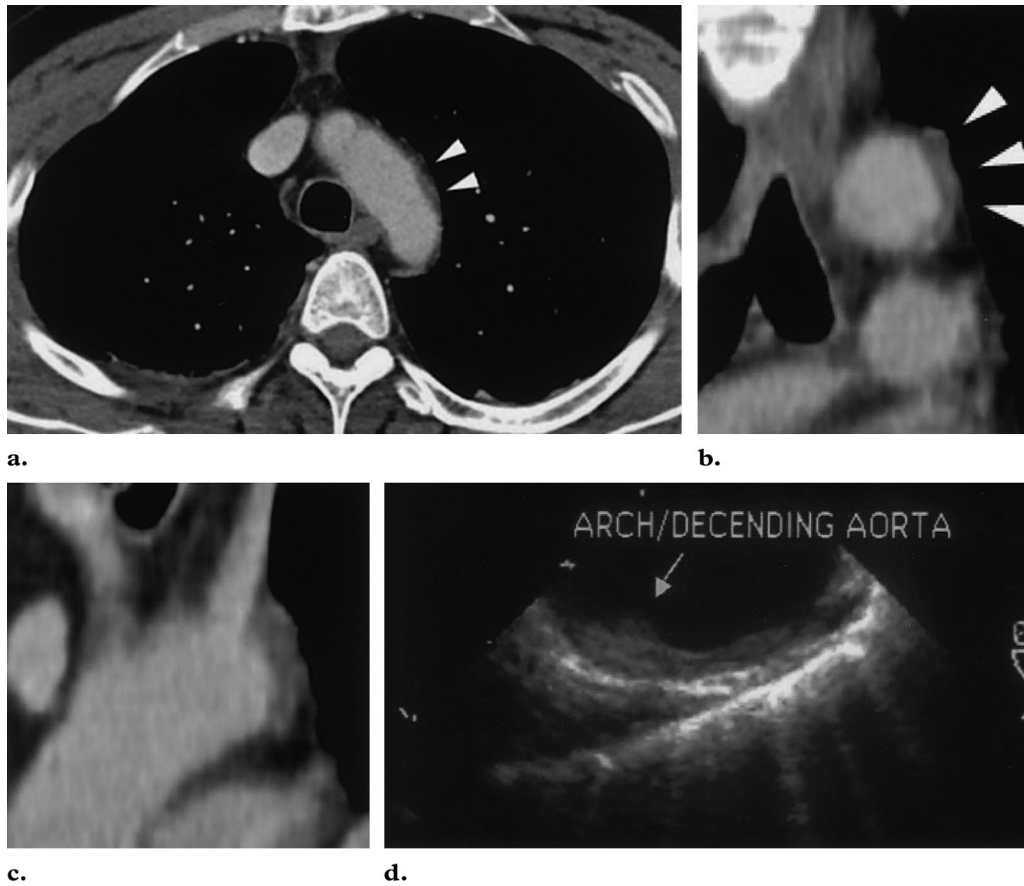
Figure 5. Acute intramural hematoma of the aorta in a 45-year-old man with blunt thoracic trauma from a traffic accident. **(a)** Axial CT image shows a small, linear, hypoattenuating lesion along the left wall of the aortic arch (arrowheads). This lesion represents an acute intramural hematoma. **(b)** Magnified coronal reformatted image shows the hematoma, which is crescent shaped. The hematoma extends over nearly half of the circumference of the left aortic wall (arrowheads) with minimal eccentric narrowing of the lumen. **(c)** Magnified sagittal reformatted image of the origin of the left subclavian artery shows cranial extension of the hematoma into the wall of the artery. **(d)** Transesophageal echocardiogram shows the extent of the hematoma (arrow), which extends into the proximal descending aorta. (Fig 5d courtesy of R. Jenni, MD, University Hospital Zurich, Switzerland.)
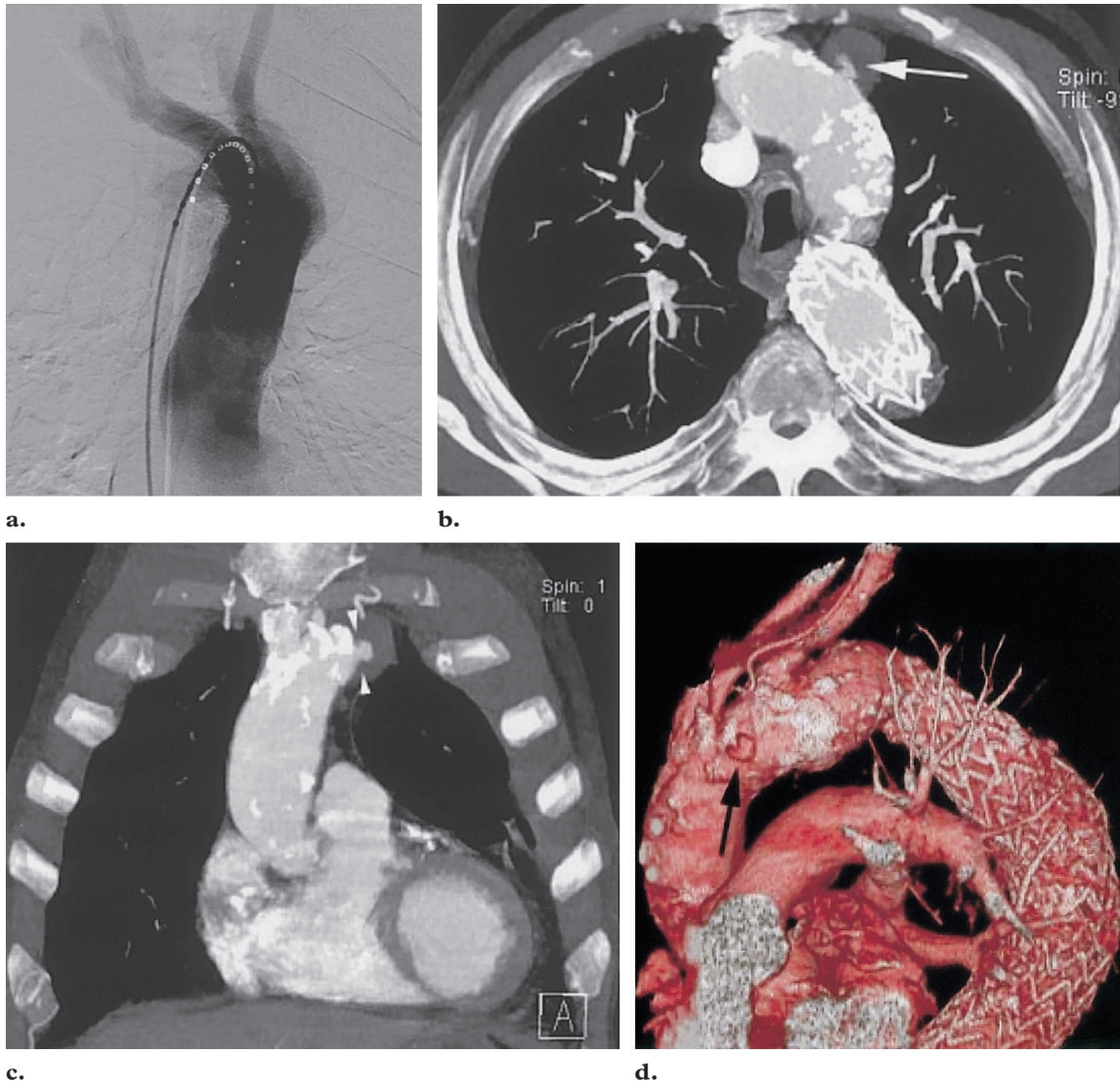
Figure 6. Pseudoaneurysm of the ascending aorta 2 weeks after endovascular repair of a descending aortic aneurysm in a 78-year-old man with severe arteriosclerosis. **(a)** Anteroposterior angiogram obtained at the time of the endovascular procedure shows no pseudoaneurysm. **(b)** Axial thin-slab MIP image shows a partially thrombosed pseudoaneurysm originating from the ascending aorta (arrow). **(c)** Coronal thin-slab MIP image shows the pseudoaneurysm as a saccular outpouching, which is demarcated from the aortic lumen by a collar (arrowheads). **(d)** Sagittal volume rendered image shows severe arteriosclerosis, a stent-graft in the descending aorta, and the perfused region of the pseudoaneurysm (arrow).

intimal injury inflicted during the deployment of the device (38,39). These pseudoaneurysms that may develop distant to the stent-graft can be accurately diagnosed with multirow CT angiography (Fig 6).

Injuries Due to Swan-Ganz Catheters

In 1970, Swan and colleagues (41) described the use of a flow-directed, balloon-tipped catheter for cardiac catheterization and cannulation of the pulmonary artery. Since then, Swan-Ganz catheters have become widely accepted and have proved to be extremely helpful in the treatment of critically ill patients. However, the use of the

catheter is not without risk, as a wide range of complications have been reported (42,43). The complications can be categorized as those of the initial venous cannulation (eg, subclavian or carotid artery laceration, carotid-jugular fistulas, pneumothorax, thoracic duct laceration, phrenic nerve injury, air embolism, and endotracheal tube cuff rupture) and those due to the catheter itself (eg, arrhythmia, infection, valvular damage, thrombosis, and pulmonary infarction).

A serious complication is pulmonary artery rupture with hemorrhage and/or pseudoaneurysm formation (42). Some patients with pulmonary artery rupture secondary to Swan-Ganz catheter manipulation remain asymptomatic and present with a new nodule or infiltrate on chest radio-

a.
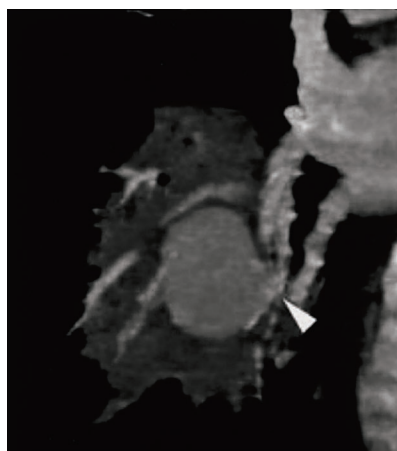
b.
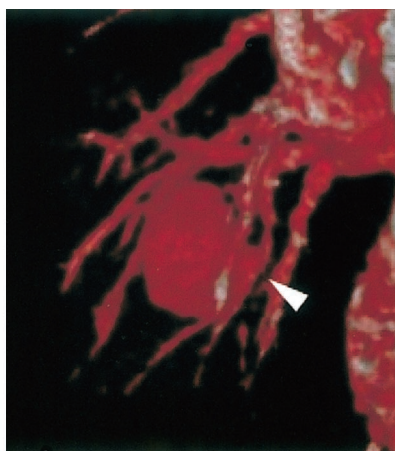
c.
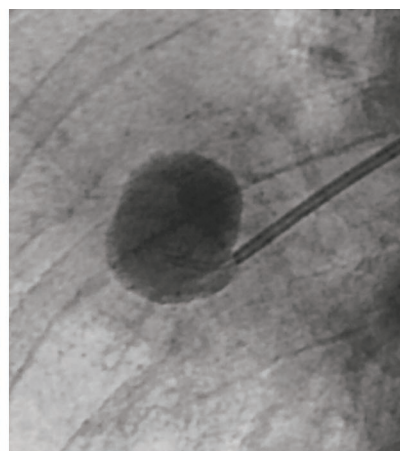
d.

Figure 7.   Catheter injury in a 58-year-old woman with hemoptysis after aortic valve replacement followed by placement of a Swan-Ganz catheter. **(a)** Axial CT image shows a pseudoaneurysm of a right pulmonary vessel. The pseudoaneurysm is contained by consolidated lung parenchyma. **(b, c)** Coronal thin-slab MIP **(b)** and coronal volume rendered **(c)** images show the feeding artery at the inferomedial border of the pseudoaneurysm (arrowhead). **(d)** Anteroposterior angiogram obtained with superselective injection of contrast medium shows the pseudoaneurysm and its feeding artery. The pseudoaneurysm was successfully treated with coil embolization.

graphs, whereas others present with the classic symptom of hemoptysis. In patients who survive the initial onset of hemoptysis, the formation of a pseudoaneurysm has been reported to occur between minutes and 7 months later (44). Thrombus formation and compressed lung parenchyma usually contain the pseudoaneurysm and thus prevent hemorrhage.

Contrast-enhanced CT has been advocated by many as the noninvasive procedure of choice in diagnosing pseudoaneurysms of the pulmonary artery (42). The pseudoaneurysm appears as an enhancing mass in continuity with an adjacent vessel (Fig 7). Occasionally, a partially thrombosed lumen can be seen. Guttentag and colleagues (45) have described two cases in which CT scans demonstrated a sharply circumscribed nodule surrounded by a halo of faint attenuation.

Although multirow CT angiography is an excellent diagnostic modality for detecting pulmonary artery pseudoaneurysms, angiography remains the standard of reference. At angiography, pseudoaneurysms appear as an extravascular collection of contrast material in continuity with a branch of the pulmonary artery (Fig 7). Catheter

angiography is not limited to just diagnostics but can also be applied for treatment (eg, endovascular embolization).

Complications of Central Venous Cannulation

Dependable venous access to the vascular system is essential in the treatment and management of critically ill patients. Many complications of the subclavian approach to central venous cannulation have been described as occurring early or late (46,47). Early complications include subclavian artery puncture, malposition, cardiac arrhythmias, localized hematoma, pneumothorax, hemothorax, and air embolism, whereas late complications include infection, thrombosis, embolism, and mediastinal hemorrhage or pericardial effusion due to erosion of the catheter through the great veins or right heart.

The symptoms and physical signs of cardiac tamponade vary considerably, depending on the amount of blood and clot in the pericardial cavity. Patients experiencing agitation, shortness of

a.

b.

c.
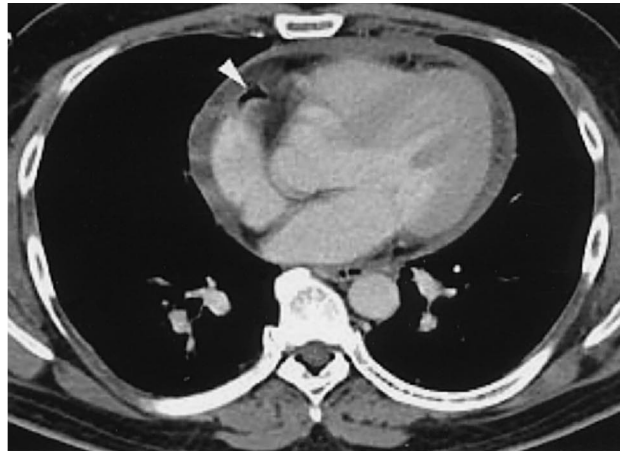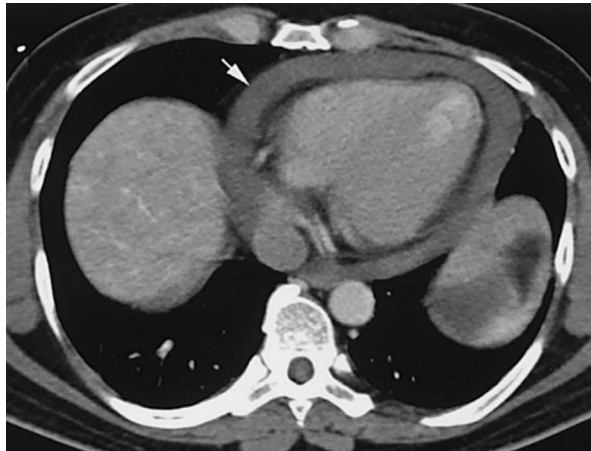
Figure 8.   Hemopericardium in a 23-year-old man with non-Hodgkin lymphoma who experienced acute retrosternal pain and dyspnea after central venous cannulation. **(a, b)** Axial CT images show hemopericardium (arrow in **a**) and small collections of extraluminal air ventral to the distal superior vena cava (arrowhead in **b**). These findings suggest that a perforation has occurred. **(c)** Coronal thin-slab MIP image shows the location of the central venous catheter after correction of the complication.

breath, and a deteriorating level of consciousness may progress rapidly to deep coma and death. The classic triad of Beck—that is, distended neck veins, arterial hypotension, and muffled heart sounds—may be present in only about 30% of patients (47). The immediate treatment of cardiac tamponade is pericardiocentesis (47). If this is unsuccessful, emergency thoracotomy should be undertaken without delay.

At CT, hemopericardium can be easily recognized as a circumferential hyperattenuating pericardial effusion (Fig 8), possibly with evidence of cardiac chamber compression. In some cases, extravascular air accumulation suggesting vessel erosion can be demonstrated. However, the presence of extravascular air does not necessarily suggest that the perforation occurred at that site.

Complications of Pacemaker Implantation

The rate of implantation of pacemakers and implantable cardioverter-defibrillators is ever-increasing. The relative ease of device implantation, which makes use of a relatively simple, expeditious, percutaneous approach without the requirements of general anesthesia or long recuperation times, has fueled enthusiasm for

implantation. However, the complication risk is not to be underestimated. A recent publication reported an acute pacemaker implant complication rate of 4%–5% (48).

Less dramatic complications include trauma to the great veins above the pericardial reflection, causing bleeding directly into the mediastinum. A more serious complication is ventricular perforation, which almost always occurs in the cardiac chamber during lead manipulation or fixing of a lead screw, with consequent bleeding into the pericardial space (48). The most devastating complication is cardiac tamponade, which requires prompt diagnosis and percutaneous pericardiocentesis, possibly followed by surgical intervention if the bleeding persists (49). Confirmation of the diagnosis is obtained by emergent bedside transthoracic echocardiography or by emergency CT.

a.

b.
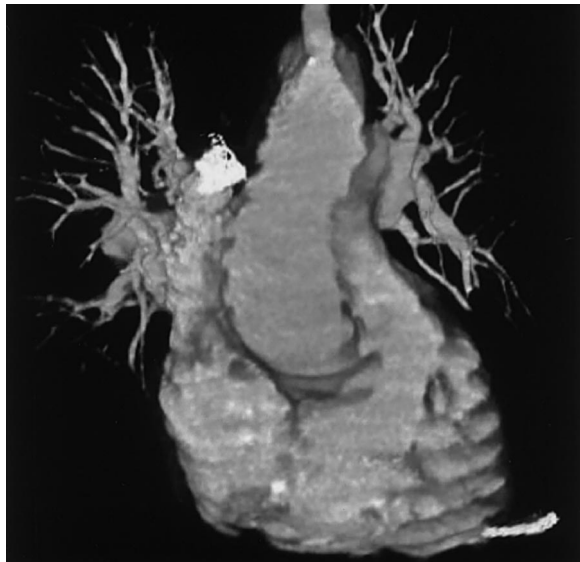
c.

Figure 9.   Ventricular perforation by a pacemaker electrode in a 66-year-old woman with acute retrosternal pain, dyspnea, and tachycardia during pacemaker implantation. **(a)** Axial thin-slab MIP image shows the tip of one pacemaker electrode outside the heart (arrowhead), whereas the other electrode is in a normal position in the left ventricle (arrow). **(b)** Coronal thin-slab MIP image shows that one electrode is in the correct location, whereas the other electrode has perforated the floor of the right ventricle (arrow). **(c)** Coronal volume rendered image shows the tip of the perforating electrode. Note the pronounced artifacts due to cardiac motion, which are one of the disadvantages of non–electrocardiographically gated CT.

At CT, hemopericardium can be easily recognized, and it should be possible to delineate the exact course and location of the perforating pacemaker electrodes. Figure 9 shows a perforation of the right ventricular wall by a pacemaker electrode. In cases of subtle right ventricular perforation, cardiac motion artifacts may hamper a correct diagnosis with CT. In these cases, cardiac-gated CT may be indicated. The introduction of multirow CT scanners with more than 16 detector rows will allow cardiac-gated acquisitions of the entire chest within one breath hold. This will possibly become the new standard for emergency chest CT.

Complications of Percutaneous Pericardial Drainage

Drainage of the pericardial cavity is a widely applied treatment for recurrent pericardial effusion and pericardial tamponade with the following objectives: determination of the cause of pericardial effusion, decompression of the pericardial cavity, and prevention of recurrence with minimal risk and discomfort to the patient (50,51). However, the optimal treatment modality for benign or malignant pericardial effusions in patients who develop tamponade remains controversial. Ideal effusion management should ensure complete and permanent drainage and provide sufficient histologic, cytologic, and microbiologic material for diagnostic study.

Two methods are routinely used for pericardial drainage: subxiphoid pericardiostomy and percutaneous drainage. The first consists of a resection

RadioGraphics

Figure 10.   Ventricular perforation in a 35-year-old man after percutaneous pericardial drainage for exudative pericarditis. **(a)** Axial CT image shows an extensive pericardial effusion with bilateral compression of the cardiac chambers, bilateral pulmonary consolidation, and pleural effusions. Only parts of the percutaneous drainage tube can be seen. **(b, c)** Coronal **(b)** and sagittal **(c)** thin-slab MIP images show the course of the tube, which makes a loop in the pericardial cavity and perforates the right ventricle (arrowhead in **c**). The end of the tube makes contact with the interventricular septum. **(d)** Sagittal volume rendered image shows the entire course of the tube (arrowheads). The end of the tube appears to perforate the interventricular septum. This wrong impression is caused by the large slab thickness used to depict the entire course of the tube.

a.

b.

c.

d.
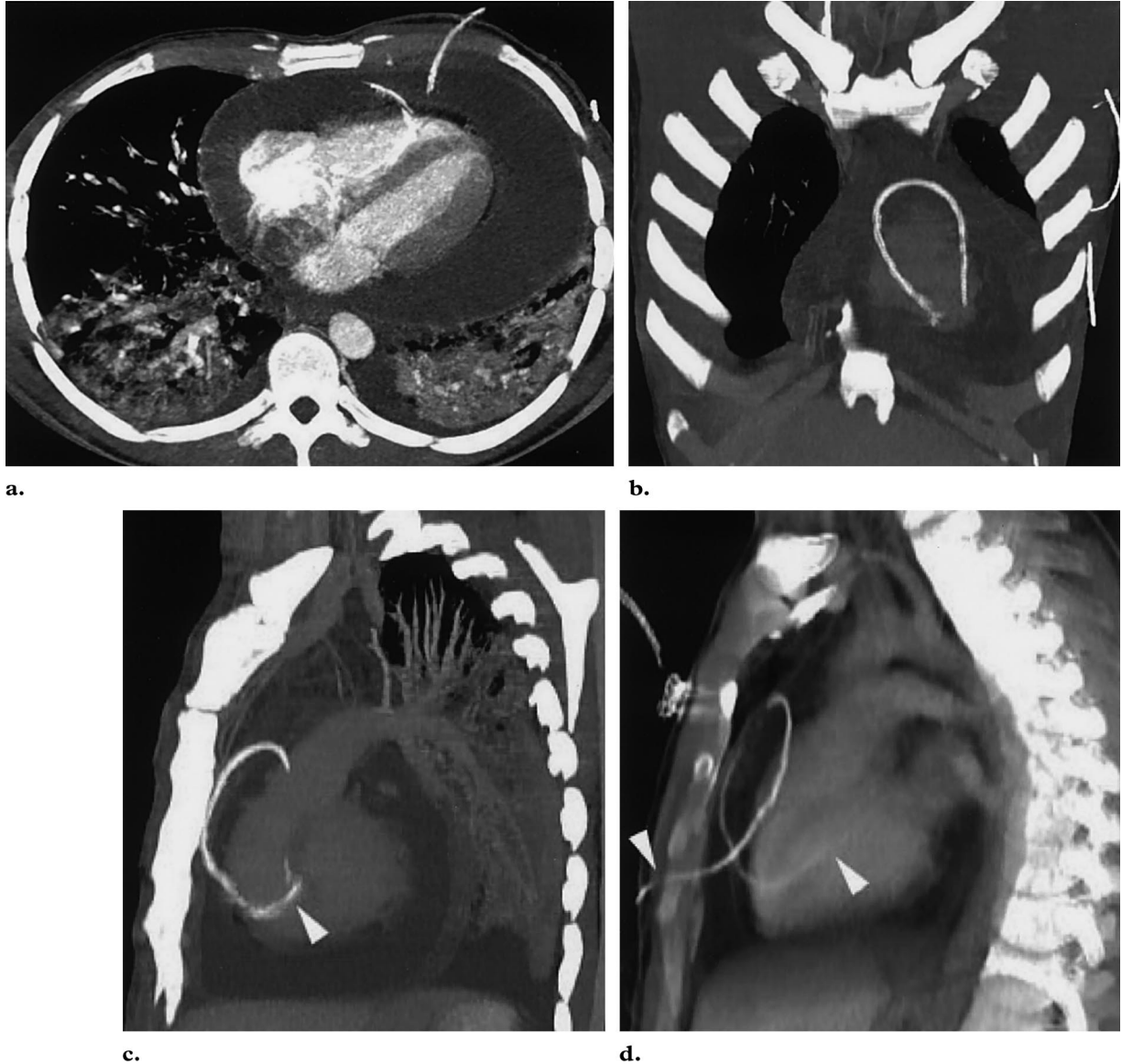
of the xiphoid process after abdominal incision, further incision of the anterior pericardium, followed by insertion of one or several tubes connected to a suction device. The latter is commonly performed by first inserting an angiographic catheter into the pericardial sac, advancing the sheath, withdrawing the needle, and advancing a guide wire followed by a dilator and a larger pigtail catheter.

Although less invasive than subxiphoid pericardiostomy, percutaneous catheter drainage is associated with increased morbidity, mortality, and effusion recurrence rates (51). The main complications after percutaneous catheter drainage include ventricular arrhythmia, pneumothoraces, and ventricular perforations. The CT signs of ventricular perforation and hemopericardium are similar to those mentioned in the case of perforating pacemaker electrodes (Fig 10).

Figure 11. Pulmonary embolism due to a lithotriptor fragment in a 31-year-old man after lithotomy for right nephro- and ureterolithiasis. **(a)** Axial volume rendered image shows a renal calculus (arrow), a percutaneous pigtail catheter, and a fragment of a lithotriptor tip (arrowhead) adjacent to the right renal vein. **(b)** Axial thin-slab MIP image obtained 2 days later shows that the fragment has migrated along the venous circulation, finally lodging in a branch of the left pulmonary artery (arrowhead). **(c)** Sagittal thin-slab MIP image shows the fragment in the pulmonary artery branch (arrowhead). **(d)** Anteroposterior angiogram shows transarterial removal of the fragment with the snare technique.
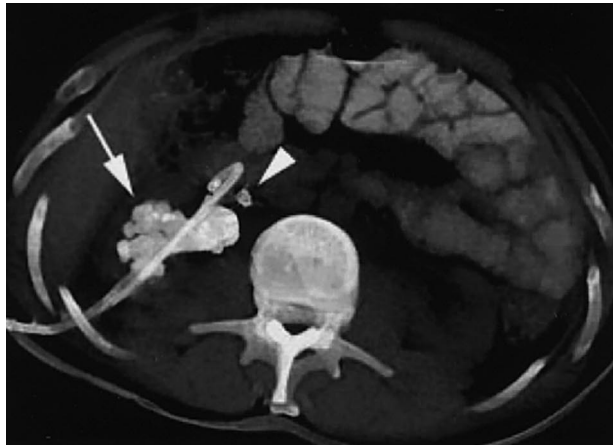
a.
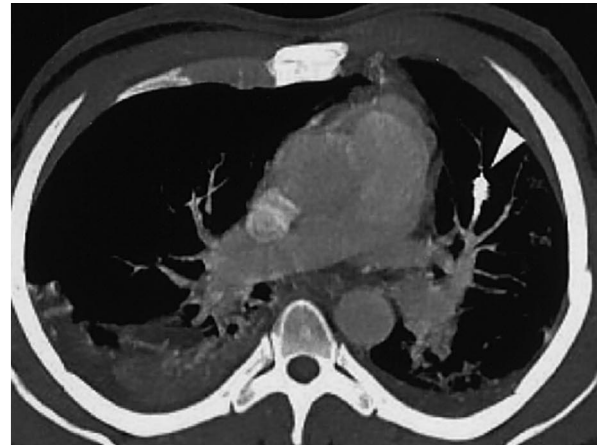
b.

c.

d.
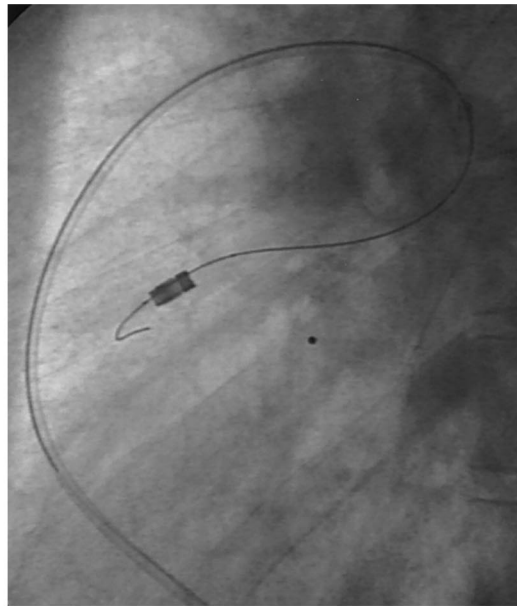
Foreign-Body Embolism

Inadvertent fracture and fragment embolization of surgical devices continue to occur despite the use of meticulous techniques (52,53). Fragments may migrate through the bloodstream and finally lodge in the vena cava, right atrium, right ventricle, or the main pulmonary artery or one of its branches. The final site of lodgment depends on the vessel configuration as well as the length, weight, and stiffness of the material. Centrally embolized foreign bodies may be associated with serious complications, but the true complication rate is unknown due to the lack of large studies (52,53).

Possible complications include myocardial perforation or necrosis culminating in tamponade,

myocardial infarction, valvular perforation, arrhythmia, and cardiac arrest (53). The foreign body can act as a nidus for thrombus formation with resultant pulmonary embolism. Infectious complications include endocarditis, secondary infection of a thrombus, mycotic aneurysms, and pulmonary abscesses. Mortality depends on the duration of the embolization as well as on the site of lodgment of the embolized foreign body. CT should allow precise localization of foreign bodies in relation to the arterial and venous vessel system, aiding surgeons and interventional radiologists in their recovery (Fig 11).

RadioGraphics

Conclusions

Multirow CT angiography is a fast, safe, and non-invasive imaging technique. In combination with two- and three-dimensional postprocessing techniques, it often clarifies complex vascular and nonvascular anatomy. Therefore, multirow CT angiography is the modality of choice for the assessment of thoracic vascular emergencies after blunt and iatrogenic trauma in the emergency setting. A well-adjusted scanning protocol consisting of a thin collimation and triggered intravenous contrast material injection is absolutely mandatory. On the other hand, the radiologist must always be aware of the weakness of this imaging modality with regard to detection of low-flow hemorrhage and assessment of small-vessel disease. Future technical developments such as further increases in axial resolution combined with intelligent dose modulation protocols may help strengthen the role of CT in the assessment of thoracic vascular emergencies.

References

1. Roos JE, Willmann JK, Weishaupt D, Lachat M, Marincek B, Hilfiker PR. Thoracic aorta: motion artifact reduction with retrospective and prospective electrocardiography-assisted multi-detector row CT. Radiology 2002; 222:271–277.
2. Novelline RA, Rhea JT, Rao PM, Stuk JL. Helical CT in emergency radiology. Radiology 1999; 213: 321–339.
3. Calhoun PS, Kuszyk BS, Heath DG, Carley JC, Fishman EK. Three-dimensional volume rendering of spiral CT data: theory and method. RadioGraphics 1999; 19:745–764.
4. Lawler LP, Fishman EK. Multi-detector row CT of thoracic disease with emphasis on 3D volume rendering and CT angiography. RadioGraphics 2001; 21:1257–1273.
5. Kalender WA, Schmidt B, Zankl M, Schmidt M. A PC program for estimating organ dose and effective dose values in computed tomography. Eur Radiol 1999; 9:555–562.
6. Richens D, Field M, Neale M, Oakley C. The mechanism of injury in blunt traumatic rupture of the aorta. Eur J Cardiothorac Surg 2002; 21:288–293.
7. Creasy JD, Chiles C, Routh WD, Dyer RB. Overview of traumatic injury of the thoracic aorta. RadioGraphics 1997; 17:27–45.
8. Ben-Menachem Y. Rupture of the thoracic aorta by broadside impacts in road traffic and other collisions: further angiographic observations and preliminary autopsy findings. J Trauma 1993; 35: 363–367.
9. Wintermark M, Wicky S, Schnyder P. Imaging of acute traumatic injuries of the thoracic aorta. Eur Radiol 2002; 12:431–442.
10. Feczko JD, Lynch L, Pless JE, Clark MA, McClain J, Hawley DA. An autopsy case review of 142 nonpenetrating (blunt) injuries of the aorta. J Trauma 1992; 33:846–849.
11. Macura KJ, Corl FM, Fishman EK, Bluemke DA. Pathogenesis in acute aortic syndromes: aortic aneurysm leak and rupture and traumatic aortic transection. AJR Am J Roentgenol 2003; 181:303–307.
12. Mirvis SE, Shanmuganathan K, Buell J, Rodriguez A. Use of spiral computed tomography for the assessment of blunt trauma patients with potential aortic injury. J Trauma 1998; 45:922–930.
13. Wicky S, Wintermark M, Schnyder P, Capasso P, Denys A. Imaging of blunt chest trauma. Eur Radiol 2000; 10:1524–1538.
14. Patel NH, Stephens KE Jr, Mirvis SE, Shanmuganathan K, Mann FA. Imaging of acute thoracic aortic injury due to blunt trauma: a review. Radiology 1998; 209:335–348.
15. Gavant ML. Helical CT grading of traumatic aortic injuries: impact on clinical guidelines for medical and surgical management. Radiol Clin North Am 1999; 37:553–574.
16. Rogers FB, Osler TM, Shackford SR. Aortic dissection after trauma: case report and review of the literature. J Trauma 1996; 41:906–908.
17. Ono M, Yagyu K, Furuse A, Kotsuka Y, Kubota H. A case of Stanford type A acute aortic dissection caused by blunt chest trauma. J Trauma 1998; 44:543–544.
18. Gammie JS, Katz WE, Swanson ER, Peitzman AB. Acute aortic dissection after blunt chest trauma. J Trauma 1996; 40:126–127.
19. Mimasaka S, Yajima Y, Hashiyada M, Nata M, Oba M, Funayama M. A case of aortic dissection caused by blunt chest trauma. Forensic Sci Int 2003; 132:5–8.
20. Fisher RG, Hadlock F. Laceration of the thoracic aorta and brachiocephalic arteries by blunt trauma: report of 54 cases and review of the literature. Radiol Clin North Am 1981; 19:91–110.
21. Perchinsky M, Gin K, Mayo JR. Trauma-associated dissection of the thoracic aorta. J Trauma 1998; 45:626–629.
22. Bashar AH, Kazui T, Washiyama N, et al. Stanford type A aortic dissection after blunt chest trauma: case report with a reflection on the mechanism of injury. J Trauma 2002; 52:380–381.
23. Faraci RM, Westcott JL. Dissecting hematoma of the aorta secondary to blunt chest trauma. Radiology 1977; 123:569–574.
24. Yoshida S, Akiba H, Tamakawa M, et al. Thoracic involvement of type A aortic dissection and intramural hematoma: diagnostic accuracy—comparison of emergency helical CT and surgical findings. Radiology 2003; 228:430–435.

25. Lauwers G, Nevelsteen A, Daenen G, Lacroix H, Suy R, Frijns JP. Ehlers-Danlos syndrome type IV: a heterogeneous disease. Ann Vasc Surg 1997; 11:178–182.

26. Cikrit DF, Miles JH, Silver D. Spontaneous arterial perforation: the Ehlers-Danlos specter. J Vasc Surg 1987; 5:248–255.

27. Beighton P, De Paepe A, Steinmann B, Tsipouras P, Wenstrup RJ. Ehlers-Danlos syndromes: revised nosology, Villefranche, 1997. Ehlers-Danlos National Foundation (USA) and Ehlers-Danlos Support Group (UK). Am J Med Genet 1998; 77:31–37.

28. Vilacosta I, Roman JA. Acute aortic syndrome. Heart 2001; 85:365–368.

29. Macura KJ, Corl FM, Fishman EK, Bluemke DA. Pathogenesis in acute aortic syndromes: aortic dissection, intramural hematoma, and penetrating atherosclerotic aortic ulcer. AJR Am J Roentgenol 2003; 181:309–316.

30. Vilacosta I, San Roman JA, Ferreiros J, et al. Natural history and serial morphology of aortic intramural hematoma: a novel variant of aortic dissection. Am Heart J 1997; 134:495–507.

31. Raab BW, Vosshenrich R, Fischer U, Funke M, Grabbe E. Intramural hematomas of the aorta. Radiologe 2001; 41:653–659.

32. Choi SH, Choi SJ, Kim JH, et al. Useful CT findings for predicting the progression of aortic intramural hematoma to overt aortic dissection. J Comput Assist Tomogr 2001; 25:295–299.

33. Goarin JP, Cluzel P, Gosgnach M, Lamine K, Coriat P, Riou B. Evaluation of transesophageal echocardiography for diagnosis of traumatic aortic injury. Anesthesiology 2000; 93:1373–1377.

34. Dyer DS, Moore EE, Mestek MF, et al. Can chest CT be used to exclude aortic injury? Radiology 1999; 213:195–202.

35. Dyer DS, Moore EE, Ilke DN, et al. Thoracic aortic injury: how predictive is mechanism and is chest computed tomography a reliable screening tool? A prospective study of 1,561 patients. J Trauma 2000; 48:673–682; discussion 682–683.

36. Dake MD, Miller DC, Semba CP, Mitchell RS, Walker PJ, Liddell RP. Transluminal placement of endovascular stent-grafts for the treatment of descending thoracic aortic aneurysms. N Engl J Med 1994; 331:1729–1734.

37. Bethuyne N, Bove T, Van den Brande P, Goldstein JP. Acute retrograde aortic dissection during endovascular repair of a thoracic aortic aneurysm. Ann Thorac Surg 2003; 75:1967–1969.

38. Kato N, Hirano T, Kawaguchi T, et al. Aneurysmal degeneration of the aorta after stent-graft repair of acute aortic dissection. J Vasc Surg 2001; 34:513–518.

39. Murgo S, Dussaussois L, Golzarian J, et al. Penetrating atherosclerotic ulcer of the descending thoracic aorta: treatment by endovascular stent-graft. Cardiovasc Intervent Radiol 1998; 21:454–458.

40. Chen FH, Shim WH, Chang BC, Park SJ, Won JY, Lee do Y. False aneurysms at both ends of a descending thoracic aortic stent-graft: complication after endovascular repair of a penetrating atherosclerotic ulcer. J Endovasc Ther 2003; 10:249–253.

41. Swan HJ, Ganz W, Forrester J, Marcus H, Diamond G, Chonette D. Catheterization of the heart in man with use of a flow-directed balloon-tipped catheter. N Engl J Med 1970; 283:447–451.

42. Poplausky MR, Rozenblit G, Rundback JH, Crea G, Maddineni S, Leonardo R. Swan-Ganz catheter-induced pulmonary artery pseudoaneurysm formation: three case reports and a review of the literature. Chest 2001; 120:2105–2111.

43. DeLima LG, Wynands JE, Bourke ME, Walley VM. Catheter-induced pulmonary artery false aneurysm and rupture: case report and review. J Cardiothorac Vasc Anesth 1994; 8:70–75.

44. You CK, Whatley GS. Swan-Ganz catheter-induced pulmonary artery pseudoaneurysm: a case of complete resolution without intervention. Can J Surg 1994; 37:420–424.

45. Guttentag AR, Shepard JA, McLoud TC. Catheter-induced pulmonary artery pseudoaneurysm: the halo sign on CT. AJR Am J Roentgenol 1992; 158:637–639.

46. Kaye CG, Smith DR. Complications of central venous cannulation. BMJ 1988; 297:572–573.

47. Forauer AR, Dasika NL, Gemmete JJ, Theoharis C. Pericardial tamponade complicating central venous interventions. J Vasc Interv Radiol 2003; 14:255–259.

48. Tobin K, Stewart J, Westveer D, Frumin H. Acute complications of permanent pacemaker implantation: their financial implication and relation to volume and operator experience. Am J Cardiol 2000; 85:774–776, A9.

49. Pavia S, Wilkoff B. The management of surgical complications of pacemaker and implantable cardioverter-defibrillators. Curr Opin Cardiol 2001; 16:66–71.

50. Dosios T, Theakos N, Angouras D, Asimacopoulos P. Risk factors affecting the survival of patients with pericardial effusion submitted to subxiphoid pericardiostomy. Chest 2003; 124:242–246.

51. Allen KB, Faber LP, Warren WH, Shaar CJ. Pericardial effusion: subxiphoid pericardiostomy versus percutaneous catheter drainage. Ann Thorac Surg 1999; 67:437–440.

52. Grabenwoeger F, Bardach G, Dock W, Pinterits F. Percutaneous extraction of centrally embolized foreign bodies: a report of 16 cases. Br J Radiol 1988; 61:1014–1018.

53. Thanigaraj S, Panneerselvam A, Yanos J. Retrieval of an IV catheter fragment from the pulmonary artery 11 years after embolization. Chest 2000; 117:1209–1211.